

PHYSICS WITH COSMIC NEUTRINOS, PEV TO ZEV

THOMAS J. WEILER

Department of Physics & Astronomy, Vanderbilt University, Nashville, TN 37235 USA
E-mail: tom.weiler@vanderbilt.edu

Neutrinos offer a particularly promising eye on the extreme Universe. Neutrinos are not attenuated by intervening radiation fields such as the Cosmic Microwave Background, and so they are messengers from the very distant and very young phase of the universe. Also, neutrinos are not deflected by cosmic magnetic fields, and so they should point to their sources. In addition, there are particle physics aspects of neutrinos which can be tested only with cosmic neutrino beams. After a brief overview of highest-energy cosmic ray data, and the present and proposed experiments which will perform neutrino astronomy, we discuss two particle physics aspects of neutrinos. They are possible long-lifetime decay of the neutrino, and a measurement of the neutrino-nucleon cross-section at a CMS energy orders of magnitude beyond what can be achieved with terrestrial accelerators. Measurement of an anomalously large neutrino cross-section would indicate new physics (e.g. low string-scale, extra dimensions, precocious unification), while a smaller than expected cross-section would reveal an aspect of QCD evolution. We then discuss aspects of neutrino-primary models for the extreme-energy (EE) cosmic ray data. Primary neutrinos in extant data are motivated by the directional clustering at EE reported by the AGASA experiment. We discuss the impact of the strongly-interacting neutrino hypothesis on lower-energy physics via dispersion relations, the statistical significance of AGASA directional clustering, and the possible relevance of the Z-burst mechanism for existing EE cosmic ray data.

1 Introduction

Detection of ultrahigh-energy neutrinos is one of the important challenges of the next generation of cosmic ray detectors. Their discovery will mark the advent of neutrino astronomy, allowing the mapping on the sky of the most energetic, and most distant, sources in the Universe. In addition, detection of extreme-energy (EE) neutrinos, those at 10^{20} eV and beyond, may help resolve puzzles associated with the giant air-shower events observed with energies beyond the Greisen-Zatsepin-Kuzmin (GZK) limit of $E_{\text{GZK}} \equiv 5 \times 10^{19}$ eV. In this context, neutrino observations may validate Z-bursts, topological defects, superheavy relic particles, new strong-interactions, *etc.*

Measurement of the neutrino cross-section itself at EE is of considerable importance to particle physics. Our highest-energy knowledge of the neutrino-nucleon cross-section comes from the HERA experiment, at a CMS energy of 0.2 TeV. The CMS energy for a CR of energy $E = 10^{20} E_{20}$ eV on an air nucleus is $\sqrt{s} = 0.5 \sqrt{E_{20}}$ PeV. This can be compared to the values of terrestrial hadron accelerators, 2 TeV at Fermilab, and 14 TeV to occur at CERN's LHC. Furthermore, if the primary CR is a neutrino, its energy is not shared among partons, so its "reach" is even larger than the comparison with Fermilab and the LHC indicates. Estimates of the cross-section at 10^{20} eV require QCD extrapolations over three orders of magnitude beyond HERA in CMS energy. Thus, a measurement of the cross-section at 10^{20} eV will test QCD with a large lever arm. Additionally, there may well be new non-SM physics revealing itself in the neutrino sector at

EE, arising from new physics thresholds not accessible to terrestrial accelerators. Needless to say, the value of the cross-section is also crucial to the future evolution of “neutrino telescope” detectors, for the neutrino event rate is proportional to this cross-section (more on this later).

And finally, we note that the stability of the neutrino is best tested with PeV cosmic neutrinos. The “cosmic” aspect guarantees a long decay path, while the PeV energy is a compromise between minimizing the boost factor $\gamma = E/m$ and ensuring events from extragalactic rather than atmospheric sources.

Several sources of neutrinos with PeV to ZeV (10^{21} eV) energies are possible, ranging conservatively from AGNs and GRBs, to exotic top-down production. The latter may in principle even provide energies up to the grand-unified mass of $\sim 10^{24}$ eV. A nice review of sources, classified according to their speculative nature, was given a few years ago by Protheroe.¹ Some of the most recent ideas for EE neutrino sources are discussed in our later section 6 on Z-bursts.

In addition to the flux of neutrinos produced in cosmic engines, there is also a reasonably guaranteed prediction for a flux of “GZK neutrinos” in the energy range 10^{15} to 10^{20} eV, based on the observed flux of cosmic ray (CR) protons at and above the GZK limit. These neutrinos result from the decay of charged pions photo-produced by the interaction of super-GZK nucleons on the CMB background. This flux is expected to peak in the decade 10^{17} to 10^{18} eV for uniformly-distributed proton sources, and around 10^{19} eV for “local” sources within ~ 50 Mpc of earth.²

On the experimental side, past observations of EE cosmic rays have been made by the Volcano Ranch, Haverah Park, AKENO, and Fly’s Eye experiments.³ The record energy, held by the Fly’s Eye event of a decade ago, is 3×10^{20} eV, or 50 Joules. This truly macroscopic amount of energy equals that in a professional baseball pitcher’s fastball, which consists of 10^{27} nucleons. This latter comment shows that somehow Nature is 10^{27} times more efficient at acceleration than is the human arm.

Most of the catalogued EE events come from the AGASA experiment, the successor to AKENO. The HiRes experiment, the successor to Fly’s Eye, has an exposure similar to AGASA, but an EE event rate lower by almost an order of magnitude. The discrepancy between these two experiments is shown in Fig. 1. There is clearly a systematic error in the energy assignments of (at least) one of the experiments. It has been noted, and is somewhat evident in the figure, that even the spectral dip (“ankle”) occurs at different energies in the two experiments. The AGASA experiment uses ground-based scintillator to measure showers, whereas HiRes uses optics to measure the near-UV light emitted by atmospheric N_2 excited by the passing shower. Fortunately, both measurement techniques will be present in the much larger AUGER experiment under construction in the high plateau of Argentina. In this experiment, simultaneous measurement of the same shower with both techniques will allow a cross-check of systematics effects, thereby settling in the next two years the issue of AGASA vs. HiRes. De Marco et al.⁴ give a quantitative appraisal of the AGASA vs. HiRes discrepancy, and the resolving potential of AUGER, and ultimately, of the “Extreme Universe Space Observatory” (EUSO) experiment.⁵ It is worth noting that if the lower HiRes rate turns out to

be correct, and even if the GZK cutoff is realized, the region above E_{GZK} remains a fertile arena for new physics. The depletion or total absence of nucleon primaries in this energy region would constitute a background free playground for the discovery of new primary particles, such as neutrinos, supersymmetric particles,⁶ magnetic monopoles,⁷ and any other exotic quanta. Moreover, the MFP for photons above 10^{21} rapidly increases to ~ 100 Mpc. This means that if there are sources of such energetic photons, they should be unmasked by the proposed larger aperture experiments.

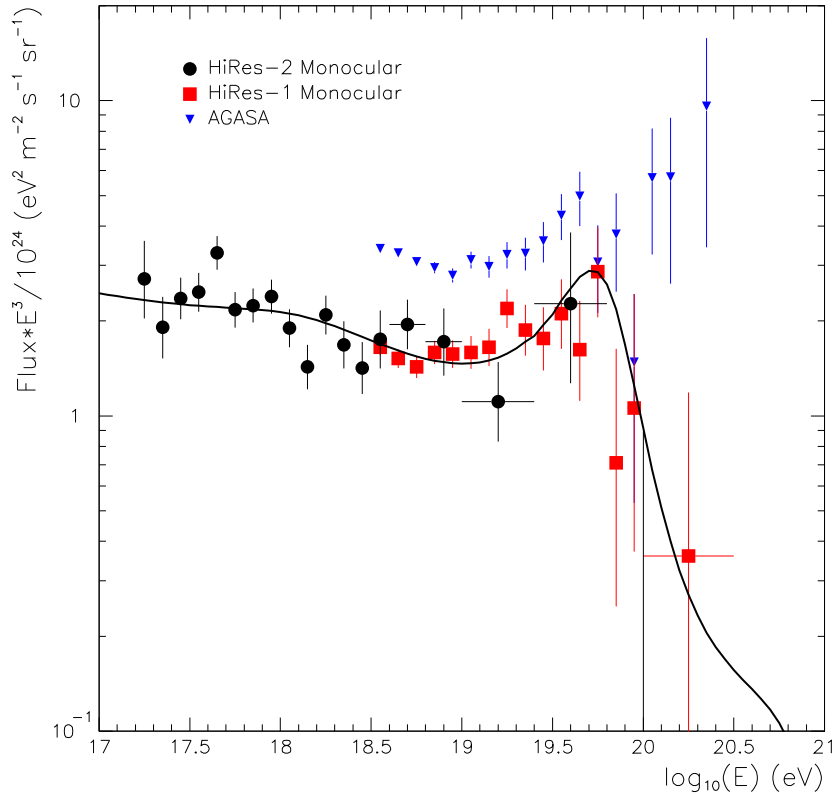


Figure 1. E^3 times the UHE Cosmic Ray Flux, with data from HiRes and AGASA (from T. Abu-Zayyad et al., HiRes Collaboration Also shown is a fit to the HiRes data of a uniform cosmic distribution of sources cutoff at $E = 10^{21}$ eV and subject to e^+e^- losses and the GZK photo-pion absorption mechanism. Not shown here is the Fly's Eye event at 3×10^{20} eV.

The EUSO experiment will mount a two meter Fresnel lens on the International Space Station (ISS), 400 km above the earth. The lens will look down on the

earth’s atmosphere, and focus the near-UV N_2 fluorescence emitted in air-shower cascades occurring in the moonless night sky. EUSO is scheduled for deployment in early 2009. Eventually, the free-flying multi-satellite experiment “OWL” may follow EUSO. In terms of US states, the Auger field of view may eventually equal the area of Rhode Island, while EUSO and OWL may equal Texas, or more. The target-mass of atmosphere available to EUSO is a teraton. For these space-based experiments, the $1/r^2$ loss at the 400-500 km height limits their sensitivity to events with energy above $\sim 10^{19}$ eV, thereby providing a natural filter to select only the most extreme-energy CRs.

The ICECUBE experiment is optimized to measure the neutrino flux at a PeV and above. It consists of strings of optical modules triggering on the Cerenkov light emitted by showers and muons in a gigaton of Antarctic Ice. This experiment builds on AMANDA, the proof-of-principle prototype experiment presently operating in South Polar ice. ICECUBE is funded, and is expected to be fully arrayed near the end of this decade. Prototypes for ocean detectors are also under construction. These are ANTARES and NESTOR in the Mediterranean Sea. A proposed gigaton array is named NEMO, possibly to be sited off of Sicily.

The far future of EE neutrino astronomy may belong to radio frequency detectors. The idea here is that the amplitude for Cerenkov emission at a particular wavelength λ coherently sums the net charge of the shower in the length λ . Since the net charge is known to be about 20% of the total charge, and the total charge scales simply with shower energy as $\sim E/\text{GeV}$, it follows that the Cerenkov rate scales as $(E/\text{GeV})^2$ at long wavelength. Thus, radio wavelengths are tremendously favored at extreme-energy. The RICE experiment at the South Pole is a prototype for radio detection. The experiment ANITA may be the first to witness an EE cosmic neutrino event. ANITA is a balloon experiment at the South Pole, configured to detect radio signals generated by showers originating from “earth-skimming” neutrinos interacting just below the horizontal (more on earth-skimmers in section 3). Eventually, large radio arrays may be deployed with ICECUBE, or in the massive salt domes which are known to populate the underground in the southeastern US.

Another noteworthy experimental idea is the mountain-to-mountain “telescope” configured to see horizontal, neutrino-induced showers emanating from one mountain toward the lens located across the valley on the other.⁹ A useful table of many happening and proposed EE neutrino experiments, assembled by Peter Gorham, is available at http://astro.uchicago.edu/home/web/olinto/aspen/gorham_table.htm.

In what follows we develop each of the theoretical themes noted earlier in this introduction.

2 Astrophysical Test of Neutrino Decay

Neutrinos from astrophysical sources are expected to arise dominantly from the decays of pions and their muon daughters, which results in initial flavor ratios $\phi_{\nu_e} : \phi_{\nu_\mu} : \phi_{\nu_\tau}$ of nearly 1 : 2 : 0. As the cosmic neutrinos travel over many oscillation lengths, they lose their phase information (“decohere”) and arrive at

earth as an incoherent ensemble of mass eigenstates. The relative fluxes of each mass eigenstate are given by $\phi_{\nu_i} = \sum_{\alpha} \phi_{\nu_{\alpha}}^{\text{source}} |U_{\alpha i}|^2$, where $U_{\alpha i}$ are elements of the neutrino mixing matrix. For three active neutrino species there is now strong evidence to suggest that ν_{μ} and ν_{τ} are maximally mixed and $U_{e3} \simeq 0$. Consequently, the neutrino mass eigenstates are produced in the ratios $\phi_{\nu_1} : \phi_{\nu_2} : \phi_{\nu_3} = 1 : 1 : 1$, and so arrive at earth in this same ratio. Due to the newly determined values of neutrino mixing parameters with their small observational uncertainties, this ratio is robust.

It was recently shown¹⁰ that this robustness allows for sensitive tests of neutrino decay, as decay would alter the measured flavor ratios in a strong and distinctive fashion. Conversely, a measurement of ratios other than 1:1:1 can be construed as evidence for unstable neutrino mass. It was further shown that neutrino decay cannot be mimicked by either different neutrino flavor ratios at the source or other non-standard neutrino interactions. In this section we elaborate on these results.

We restrict our attention to the two body decays

$$\nu_i \rightarrow \nu_j + X \quad \text{and} \quad \nu_i \rightarrow \bar{\nu}_j + X, \quad (1)$$

for which limits are too weak to eliminate the possibility of astrophysical neutrino decay by a factor of about $10^7 \times (L/100 \text{ Mpc}) \times (10 \text{ TeV}/E)$.¹¹ Here, ν_i are neutrino mass eigenstates and X denotes a very light or massless particle, e.g. a singlet Majoron. Radiative two-body decay modes and three-body decays of the form $\nu \rightarrow \nu\nu\bar{\nu}$ need not be considered, as they are already constrained beyond what can be inferred from cosmic fluxes, by the absence of photons in appearance searches, and by bounds on anomalous $Z\nu\bar{\nu}$ couplings, respectively.

We also assume that the decays are complete, i.e. none of the decaying state arrives at earth. This is reasonable because even the shortest distances are typically hundreds of Mpc, and the typical energies in a steeply falling spectrum are not too large. The assumption of complete decay means that the distance and intensity distributions of sources need not be considered. Finally, neutrinos and antineutrinos need not be distinguished because their cross sections rapidly approach each other above 10 TeV.

First suppose that there are no detectable decay products, that is, the decaying neutrinos simply disappear. Such would be the case for decay to “invisible” daughters such as a sterile neutrino, or for decay to active daughters if the source spectrum falls sufficiently steeply with energy so that the flux of daughters with degraded energy makes a negligible contribution to the total flux at that energy. Since coherence is lost, one has for the flavor fluxes (assuming completeness: $L \gg \tau_i$),

$$\phi_{\nu_{\alpha}}(E) \longrightarrow \sum_{s,\beta} \phi_{\nu_{\beta}}^{\text{source}}(E) |U_{\beta s}|^2 |U_{\alpha s}|^2, \quad (2)$$

where the sum on s is over just the stable states.

The simplest case (and the most generic expectation) is a normal hierarchy in which both ν_3 and ν_2 decay, leaving only the lightest stable eigenstate ν_1 . In this case the flavor ratio is $U_{e1}^2 : U_{\mu 1}^2 : U_{\tau 1}^2$. Neglecting $U_{e3} = 0$, one then has

$$\phi_{\nu_e} : \phi_{\nu_{\mu}} : \phi_{\nu_{\tau}} = \cos^2 \theta_{\odot} : \frac{1}{2} \sin^2 \theta_{\odot} : \frac{1}{2} \sin^2 \theta_{\odot} \simeq 6 : 1 : 1, \quad (3)$$

where θ_\odot is the solar neutrino mixing angle, which we set to 30° . In the case of an inverted hierarchy, ν_3 is the lightest and hence stable state, and so

$$\phi_{\nu_e} : \phi_{\nu_\mu} : \phi_{\nu_\tau} = U_{e3}^2 : U_{\mu 3}^2 : U_{\tau 3}^2 = 0 : 1 : 1. \quad (4)$$

Interestingly, both cases have extreme deviations of the flavor ratio from the 1:1:1 in the absence of decays, which provides a very useful diagnostic. Assuming no new physics besides decay, a ratio of $\phi_{\nu_e} : \phi_{\nu_\mu}$ greater than 1 suggests the normal hierarchy, while a ratio smaller than 1 suggests an inverted hierarchy. It is also interesting to note that complete decay cannot reproduce 1 : 1 : 1. One of the mass eigenstates does have a flavor ratio similar to 1 : 1 : 1, but it is the heavier of the two solar states and cannot be the lightest, stable state. (A possible but unnatural exception occurs if only this state decays).

These clear and striking predictions depend strongly on the recent progress which determined the neutrino mixing parameters. In particular, it is very significant that $\theta_\odot \simeq 30^\circ$ is well below the maximal 45° , for which Eq. (3) would instead be a much less dramatic 2 : 1 : 1. In addition, $\theta_\odot < 45^\circ$ means that $\delta m_{12}^2 > 0$ and hence that ν_2 (with flavor ratios 0.7 : 1 : 1) can never be the lightest mass eigenstate. Maximal θ_{atm} and very small U_{e3} also make the predictions clearer.

Quite different ratios may result, depending on which of the mass eigenstates are unstable, the decay branching ratios, and the hierarchy of the neutrino mass eigenstates. Also, when the appearance of daughter neutrinos from the decay cannot be neglected, the equations are more complicated, but only slightly so. That case is also treated in Beacom et al,¹⁰ for both Dirac and for Majorana neutrinos. I do not treat that case here, but instead, list some possibilities for the normal hierarchy in Table I.

Table 1. Flavor ratios for various decay scenarios (normal hierarchy only).

Unstable	Daughters	Branchings	$\phi_{\nu_e} : \phi_{\nu_\mu} : \phi_{\nu_\tau}$
ν_2, ν_3	anything	irrelevant	6 : 1 : 1
ν_3	sterile	irrelevant	2 : 1 : 1
ν_3	full energy	$B_{3 \rightarrow 2} = 1$	1.4 : 1 : 1
	degraded ($\alpha = 2$)		1.6 : 1 : 1
ν_3	full energy	$B_{3 \rightarrow 1} = 1$	2.8 : 1 : 1
	degraded ($\alpha = 2$)		2.4 : 1 : 1
ν_3	anything	$B_{3 \rightarrow 1} = 0.5$	2 : 1 : 1
		$B_{3 \rightarrow 2} = 0.5$	

An important issue is whether there are other scenarios (either non-standard astrophysics or non-standard neutrino properties) that would give similar ratios. The answer is that since the mixing angles θ_\odot and θ_{atm} are both large, and since the neutrinos are produced and detected in flavor states, no initial flavor ratio can result in a measured $\phi_{\nu_e} : \phi_{\nu_\mu}$ ratio anything like that of our two main cases, 6 : 1 and 0 : 1. In terms of non-standard particle physics, decay is unique in the sense that it is “one-way”. Oscillations or magnetic moment transitions are, on the other

hand, “two-way”. Since the initial flux ratio in the mass basis is 1 : 1 : 1, magnetic moment transitions between (Majorana) mass eigenstates cannot alter this ratio, due to the symmetry between $i \rightarrow j$ and $j \rightarrow i$ transitions. However, if neutrinos have Dirac masses, magnetic moment transitions (both diagonal and off-diagonal) turn active neutrinos into sterile states, so the same symmetry is not present. Yet the process will average out at 1/2, so there is no way to leave only a single mass eigenstate.

Experimentally, the number of muon tracks and the number of showers (charged- and neutral-current combined) are accessible. The relative number of shower events to track events can be related to the most interesting quantity for testing decay scenarios, i.e., the ν_e to ν_μ ratio. The precision of the upcoming experiments, e.g. ICECUBE, should be good enough to test the extreme flavor ratios produced by decays, and thereby discover or limit neutrino decay.

3 Can’t Lose Theorem for Smaller/Larger Neutrino Cross-Section

The expected rates for neutrino observation in approved and proposed experiments are proportional to $\sigma_{\nu N}$. The grossly-extrapolated cross section at 10^{20} eV is $\sim 10^{-31}\text{cm}^2$. If Nature offers a smaller cross section, then the main detection signal proposed for UHE neutrino experiments would be compromised. On the other hand, the extrapolated cross-section may be too low, for it ignores possible contributions from new physics that may enter in the $\sim\text{TeV}$ to PeV scale accessible to CR physics but inaccessible to terrestrial accelerators.

Consider, for example, the space-based experiments EUSO and OWL. The event rate for nearly horizontal air showers (HAS) resulting from ν -air interactions in the Earth’s atmosphere is proportional to $\sigma_{\nu N}$. Fortuitously, it was recently shown¹² that the flux of up-going charged leptons (UCL) per unit surface area produced by neutrino interactions *below* the Earth’s surface is *inversely* proportional to $\sigma_{\nu N}$, as long as the neutrino absorption mean free path in Earth is small in comparison with the Earth’s radius (R_\oplus); i.e. for $\sigma_{\nu N} \gtrsim 2 \times 10^{-33}\text{cm}^2$ (see Fig. 2). This contrasts with the HAS rate proportional to $\sigma_{\nu N}$. Even when showering of the upgoing tau lepton is included, the upgoing air-shower (UAS) rate still varies inversely with the cross-section in the range of interest, and can even exceed the HAS rate by several orders of magnitude, as displayed in Fig. 3.

Taken together, up-going and horizontal rates ensure a healthy total event rate, regardless of the value of $\sigma_{\nu N}$. Moreover, by comparing the HAS and UAS rates, the neutrino-nucleon cross section can be inferred at energies as high as 10^{11} GeV or higher. This enables QCD studies at a minimum, and possibly discovery of a strong neutrino cross-section. $\sigma_{\nu N}$ may also be determinable from a measurement of the angular distribution of UCL/UAS events, in addition to the approach comparing UAS and HAS rates. One expects the angular distribution of UCL to peak near $\cos\theta_{\text{peak}} \sim (2 \langle \rho \rangle R_\oplus \sigma_{\nu N})^{-1}$.

Let us now examine the physics of upward showers in some detail. UHE neutrinos are expected to arise from pion and subsequent muon decay. These flavors oscillate and eventually decohere during their Hubble-time journey. If $|U_{\tau 3}| \simeq |U_{\mu 3}|$ are large, as inferred from the Super-Kamiokande data, then $F_{\nu_\tau} \approx \frac{1}{3}F_\nu$ is expected.

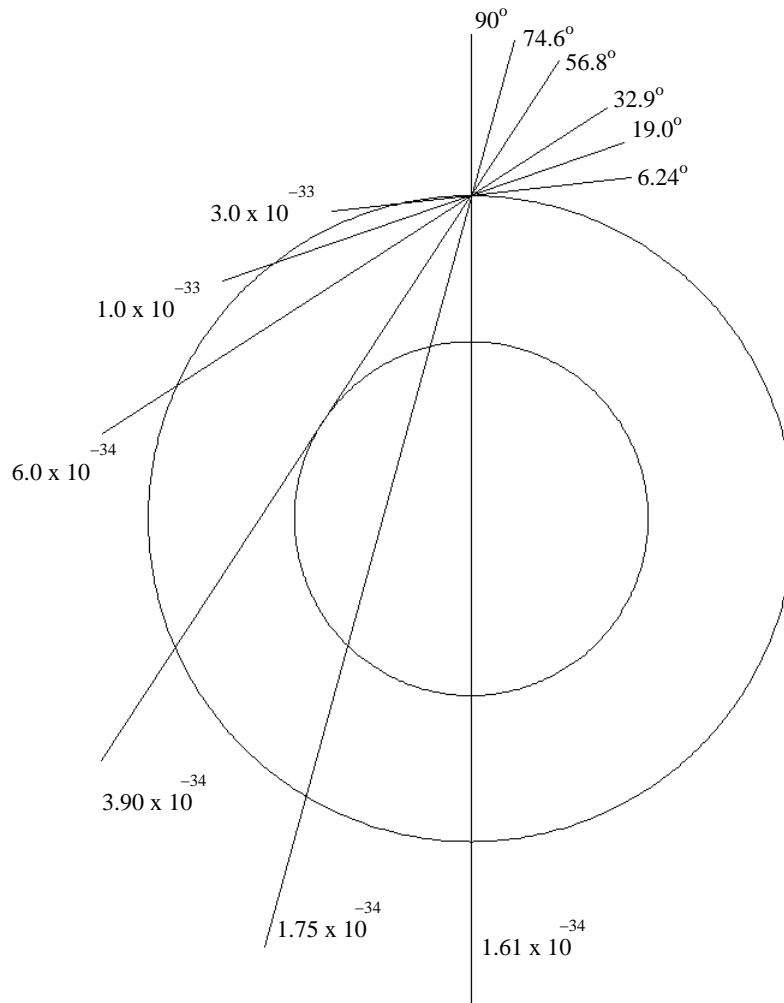


Figure 2. Neutrino MFP displayed as a chord length in the earth. Cross-section values label the various MFP's.

Because the energy-loss MFP for a τ produced in rock or water is much longer than that of a muon or electron, the produced taus have a much higher probability to emerge from the Earth and to produce an atmospheric shower. Thus, the dominant primary for initiation of UAS “earth-skimming” events is the tau neutrino. ¹³

Consider an incident tau neutrino whose trajectory cuts a chord of length l in the

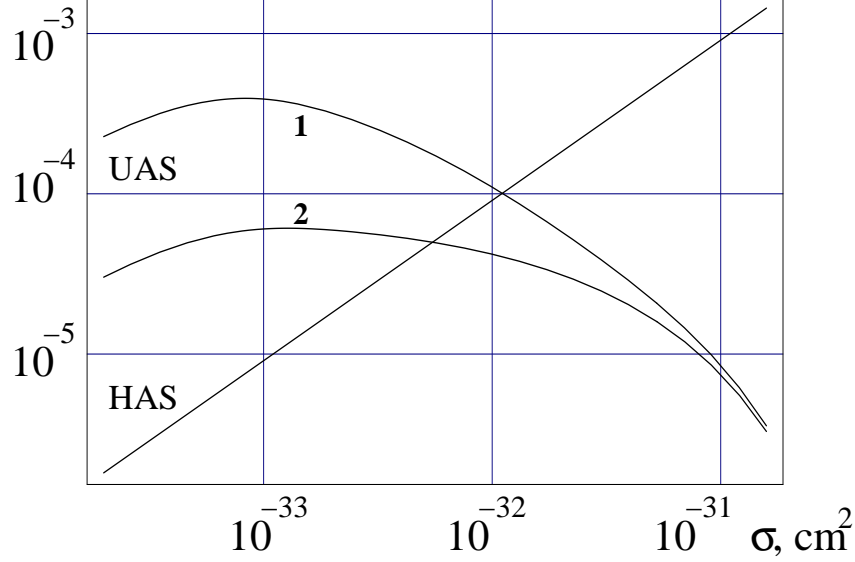


Figure 3. The air shower probability per incident tau neutrino $R_{\text{UAS}}/F_{\nu_\tau} \pi A$ as a function of the neutrino cross section (eq.(7)). The incident neutrino energy is 10^{20} eV and the assumed energy threshold for detection of UAS is $E_{\text{th}} = 10^{18}$ eV for curve 1 and 10^{19} eV for curve 2.

Earth. The probability for this neutrino to reach a distance x is $P_\nu(x) = e^{-x/\lambda_\nu}$, where $\lambda_\nu^{-1} = \sigma_{\nu N} \rho$ (the conversion from matter density to number density via N_A/gm is implicit). The probability to produce a tau lepton in the interval dx is $\frac{dx}{\lambda_\nu}$. The τ produced at point x emerges from the surface with energy $E_\tau \sim E_\nu e^{-(l-x)/\lambda_\tau}$. To produce an observable shower, one requires $P_{\tau \rightarrow \text{UAS}} = \Theta(\lambda_\tau + x - l)$, with $\lambda_\tau = (\beta_\tau \rho_{sr})^{-1} \ln(E_\nu/E_{\text{th}})$; $\beta_\tau \approx 0.8 \times 10^{-6} \text{cm}^2/\text{g}$ is the exponential energy-attenuation coefficient and E_{th} is the minimum detectable energy. Taking the product of these conditional probabilities and integrating over the interaction site x we get the probability for a tau neutrino incident along a chord of length l to produce an UCL:

$$P_{\nu_\tau \rightarrow \tau}(l) = \int_{l-\lambda_\tau}^l \frac{dx}{\lambda_\nu} e^{-x/\lambda_\nu} = (e^{\lambda_\tau/\lambda_\nu} - 1) e^{-l/\lambda_\nu}. \quad (5)$$

The emerging tau decays in the atmosphere with probability $P_d = 1 - \exp(-2R_\oplus H/c\tau_\tau l)$, where $H \approx 10$ km parametrizes the height of the atmosphere. Thus, the probability for a tau-neutrino to produce an UAS is

$$P_{\nu_\tau \rightarrow \text{UAS}}(l) = (1 - e^{-2R_\oplus H/c\tau_\tau l}) P_{\nu_\tau \rightarrow \tau}(l). \quad (6)$$

The fraction of neutrinos with chord lengths in the interval $\{l, l + dl\}$ is $\frac{l}{2R_\oplus^2} dl$. Finally, including two further geometric factors, the solid angle π for a planar detector with hemispherical sky-coverage, and the tangential surface area A of the

detector, we arrive at the rate of UCL and UAS events:

$$R_{\tau(\text{UAS})} = F_{\nu_\tau} \pi A \int_0^{2R_\oplus} \frac{l dl}{2R_\oplus^2} P_{\nu_\tau \rightarrow \tau(\text{UAS})}(l). \quad (7)$$

In Fig. 3 we show the number of expected UAS events per incoming neutrino as a function of the neutrino cross section. For comparison, we also show the number of expected HAS events per neutrino that crosses a 250 km field of view, up to an altitude of 15 km. It is clear that for the smaller values of the cross section, UAS events will outnumber HAS events, and vice versa.

We give some examples of the UAS event rates expected from a smaller neutrino cross section at 10^{20} eV, choosing $\sigma_{\nu N} = 10^{-33} \text{cm}^2$ as an example. EUSO and OWL have shower-energy thresholds $E_{\text{th}} \sim 10^{19} \text{eV}$ corresponding to curve 2 in Fig. 3, and apertures $\sim 6 \times 10^4 \text{km}^2$ and $3 \times 10^5 \text{km}^2$, respectively. These detectors should observe F_{20} and $7F_{20}$ UAS events per year, respectively (not including duty cycle); here F_{20} is the incident neutrino flux at and above 10^{20} eV in units of $\text{km}^{-2} \text{sr}^{-1} \text{yr}^{-1}$, one-third of which are ν_τ 's. Including showers from taus originating outside the field of view, and direct tau events, increases these rates, as does tilting space-based detectors toward the horizon to maximize the acceptance for events with smaller chord lengths and to allow more atmospheric path length for tau decay. The rates will also increase if E_{th} can be reduced.

Recently, it was pointed out that production of the lightest supersymmetric particle (LSP) from annihilating dark matter may present a detectable flux of LSP-CRs. ⁶ A higgsino-dominated LSP may have a cross-section as small as 10^{-2} times the SM neutrino cross-section. Such a tiny cross-section is a perfect example of what can be discovered and measured via either the UAS/HAS or the angular-dependence methods discussed here.

4 Dispersion Relations: the High-Energy/Low-Energy Connection

A neutrino primary is not subject to the GZK losses that limit cosmic nucleon propagation. However, the extrapolated neutrino-nucleon cross-section is expected to be 10^{-31}cm^2 , about 10^{-6} too small to provide the neutrino with interactions high in our atmosphere. To explain the production of the observed EE cosmic ray events with neutrino primaries, some have postulated a new strong-interaction for neutrinos above $\sim 10^{19}$ eV. The idea of a strongly-interacting neutrino is not new, but recent developments in field theory and in gravity have given new motivation to such a picture. To mimic hadronically-induced air showers, the new neutrino cross section must be of hadronic strength, $\sim 100 \text{mb}$, above $E_{\text{GZK}} = 5 \times 10^{19}$ eV. Simple perturbative calculations of single scalar or vector exchange cannot provide an acceptably fast growth of the cross-section with energy. ¹⁴ However, the modern thoughts on large TeV-scale cross-sections are much more imaginative. A plethora of new states, possibly growing exponentially in s or \sqrt{s} , is motivated by precocious unification, low-scale string theory, and modes from additional space-dimensions accessible at $\sqrt{s} \sim \text{TeV}$. Electroweak instantons are the most recent possibility. ¹⁵

Direct limits on the EE neutrino cross-section are quite weak. The vertical column density of our atmosphere is $X_v = 1033 \text{g/cm}^2$. In terms of neutrino MFP

λ_ν , this may be written $X_v/\lambda_\nu = \sigma_{\nu N}/1.6 \text{ mb}$. The horizontal slant depth X_h is 36 times larger, leading to $X_h/\lambda_\nu = \sigma_{\nu N}/44 \mu\text{b}$. Since penetrating events are not observed above us or to our side, the neutrinos must be interacting high in the atmosphere (large cross-section) or not interacting at all (small cross-section). Thus the cross-section range from $\sim 20 \mu\text{b}$ to $\sim 1 \text{ mb}$ is excluded. More quantitative analyses give similar results. ^{16,17}

A very interesting indirect limit on the EE neutrino cross-section is provided by dispersion relations. ¹⁸ Dispersion relations are rigorous, nonperturbative, and model-independent. They limit the growth of the *elastic* neutrino amplitude at low energy due to any rising cross-section at higher energies. If new physics dominates the neutrino total cross-section with a value σ^* above the lab energy E^* , then the dispersion relation determines the real part of the new strong-interaction elastic amplitude at lower energy E to be $\frac{1}{2\pi} \frac{E}{E^*} \sigma^*$. Remarkably, significantly enhanced rates may occur for elastic νN scattering at an energy seven orders of magnitude lower than the onset of a new total cross-section. ¹⁸ Such anomalous “low” energy scattering may be observable in the neutrino beams available at Fermilab and CERN, and maybe in quasi-elastic $e^- p \rightarrow \nu_e n$ scattering at HERA.

How does this magic come about? Assuming only that the scattering amplitude is analytic, there results the following dispersion relation: ¹⁸

$$\text{Re } A_\pm(E) - \text{Re } A_\pm(0) = \frac{E}{4\pi} \mathcal{P} \int_0^\infty dE' \left(\frac{\sigma_{tot}^{\nu N}(E', \pm)}{E'(E' - E)} + \frac{\sigma_{tot}^{\bar{\nu} N}(E', \pm)}{E'(E' + E)} \right) \quad (8)$$

where $A_\pm(E)$ are invariant ν - N amplitudes, labeled by the nucleon helicity, and \mathcal{P} denotes the principle value of the integral. Suppose the new physics dominates the neutrino-nucleon dispersion integral (8) for $E' \geq E^*$ as hypothesized to explain the air showers observed above the GZK limit. Assuming that σ^* is independent of helicity and energy, and obeys the Pomeranchuk theorem: $\sigma_{tot}^{\nu N}(E, \pm) - \sigma_{tot}^{\bar{\nu} N}(E, \pm) \xrightarrow{E \rightarrow \infty} 0$, the real part of the amplitude at energy E emerges:

$$\text{Re } A_\pm(E) \simeq \text{Re } A_\pm(0) + \frac{1}{2\pi} \frac{E}{E^*} \sigma^* \quad . \quad (9)$$

This result cannot be obtained in perturbation theory! $\text{Re } A_\pm(0)$ is nothing but the low energy limit of the weak interaction, $\sim \frac{G_F}{2\sqrt{2}}$. From this, we may immediately write down the ratio of the new amplitude to the SM amplitude:

$$\frac{\text{Re}A(E)_{\text{new}}}{\text{Re}A(E)_{\text{SM}}} \simeq \left(\frac{E/100 \text{ GeV}}{E^*/10^{18} \text{ eV}} \right) \left(\frac{\sigma^*}{100 \text{ mb}} \right) \quad . \quad (10)$$

It is clear from (10), and striking, that order 100% effects in the real elastic amplitudes begin to appear already at energies seven orders of magnitude below the full realization of the strong cross section.

A promising observable consequence is available from the elastic cross section, obtained from the square of the elastic amplitude. The result (8) says that if the neutrino is strongly interacting at $E^* \sim 10^{17.5} \text{ eV}$, then a factor of ten anomalous rise in the elastic cross-section is occurring at 100 GeV, a neutrino energy already available at Fermilab and CERN. Since the anomalous elastic cross-section grows quadratically with E , the anomalous event rate develops rapidly for $E > 100 \text{ GeV}$.

Thus, the event sample of a future underground/water/ice neutrino telescope optimized for TeV neutrinos could conceivably contain *1000* times more elastic neutrino events than predicted by the SM; and a telescope optimized for PeV neutrinos may contain 10^9 more elastic events. Some of the wilder brane-world cross-sections proposed for the EE neutrino are ruled out by this dispersion result.

There may be further tests of the strong-interaction hypothesis. If the neutrino develops a strong-interaction at high energy, do not the electron and the other charged-lepton $SU(2)$ -doublet partners of the neutrinos also develop a similar strong-interaction? Is there new physics in the quasi-elastic $e^-p \rightarrow \bar{\nu}_e n$ scattering channel at HERA energies? A possible enhancement in the quasi-elastic channel cannot be deduced from dispersion relations. A separate calculation can be made, however, if certain aspects of the new high-energy strong-interaction are assumed. This is presently under investigation. ¹⁹

5 Puzzles in the Extreme-Energy Cosmic Rays (EECRs)

The discoveries by the AGASA, Fly's Eye, Haverah Park, and Yakutsk collaborations of air shower events with energies above the GZK cutoff challenge the SM of particle physics and the hot big-bang model of cosmology. Not only is the mechanism of particle acceleration for such EECRs controversial, but also the propagation of EECRs over cosmic distances is problematic. As has been mentioned, however, the HiRes experiment does not confirm the prior AGASA rate for events $\sim 10^{20}$ eV. The situation will remain murky until the Auger hybrid detector provides guidance.

The famous Fly's Eye event occurred high in the atmosphere, whereas the event rate expected in the SM for early development of a neutrino-induced air shower is down from that of an electromagnetic or hadronic interaction by six orders of magnitude. On the other hand, Fig. 4 presents the AGASA evidence that the arrival directions of some of the highest-energy primaries are paired. ²⁰ Furthermore, a recent analysis of the arrival directions of the super-GZK events offers a tentative claim of a correlation with the directions of BL-Lac quasars. ²¹ This correlation, if validated with future data, and the pairing data, argue for propagating cosmic particles which are charge neutral, stable, and have a negligible magnetic moment. The neutrino emerges as the only candidate among the known particles.

Several non-neutrino solutions for the origin of the exceptional EECRs have been proposed. Magnetic caustics have been proposed as a focusing mini-lens bringing charged particles into pairs, and it is conceivable that some new physics at high energy could stabilize the neutron. With magnetic caustics one gets pairing but not pointing; with stabilized neutrons, one gets pairing and pointing. Generally, other proposed models are distinguishable from these and the neutrino scenario by the lack of pairing and pointing.

The unexpected degree of small-scale clustering observed in the highest-energy AGASA cosmic ray day has motivated a derivation of analytic formulas²² which estimate the probability of random cluster configurations. The derived formulas offer a quick study of the strong potential of HiRes, Auger, and EUSO for deciding whether any observed clustering is meaningful or random. For detailed comparison to data, this analytical approach cannot compete with Monte Carlo simulations in-

AGASA + A20

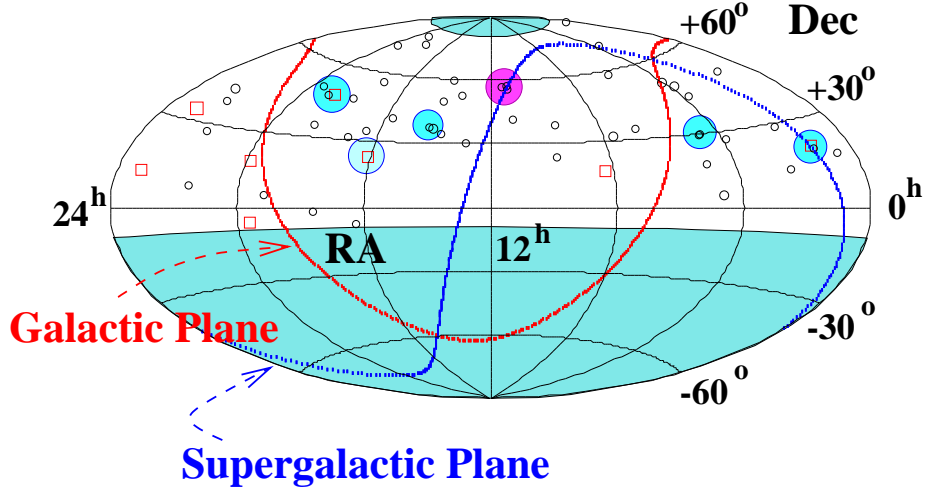


Figure 4. AGASA sky-map of the arrival directions of the highest-energy cosmic rays (from the AGASA homepage). The five light-shaded disks contain doublets, and the one darker disk contains a triplet. Disk solid angles are $\pi (\theta/2)^2$, with cone opening-angle $\theta = 2.5^\circ$.

cluding experimental systematics. Nevertheless, a recent Monte Carlo calculation²³ of joint multiplet-probabilities shows reasonably good agreement with the analytic approach presented here. (The same MC analysis also cross-correlates different energy bins to suggest that pairing is emerging only above 10^{19} eV.) The derived formulas here do offer two advantages over Monte Carlo techniques: (i) easy assessment of the significance of any observed clustering, and most importantly, (ii) an explicit dependence of cluster probabilities on the chosen angular bin-size.

To derive the combinatoric formula for the probability of various event distributions in angle, imagine that the sky coverage consists of a solid angle Ω divided into N equal angular bins, each with solid angle $\omega \simeq \pi\theta^2$ steradian. Define each event distribution by specifying the partition of the n total events into a number m_0 of empty bins, a number m_1 of single hits, a number m_2 double hits, etc. The probability to obtain a given event topology is:

$$P(\{m_j\}, n, N) = \frac{1}{N^n} \frac{N!}{m_0! m_1! m_2! m_3! \dots} \frac{n!}{(0!)^{m_0} (1!)^{m_1} (2!)^{m_2} (3!)^{m_3} \dots} \quad (11)$$

The variables in the probability are not all independent. The partitioning of events is related to the total number of events by $\sum_{j=1} j \times m_j = n$, and to the total number of bins by $\sum_{j=0} m_j = N$. Because of these constraints, one infers that the process is not described by a simple multinomial or Poisson probability

distribution. It is useful to use these constraints to rewrite the probability (11) as

$$P(\{m_j\}, n, N) = \frac{N!}{N^N} \frac{n!}{n^n} \prod_{j=0} \frac{(\overline{m}_j)^{m_j}}{m_j!}, \quad (12)$$

where

$$\overline{m}_j \equiv N \left(\frac{n}{N} \right)^j \frac{1}{j!}. \quad (13)$$

In the $n \ll N$ limit, \overline{m}_j is expected to approximate the mean number of j -plets, and eq. (12) becomes roughly Poissonian. As an approximate mean, \overline{m}_j defined in eq. (13) provides a simple estimate of cluster probabilities due to chance for the $n \ll N$ case.

Two large-number limits of interest are $N \gg n \gg 1$, and $n > N \gg 1$. With bin numbers typically $\sim 10^3$, the first limit applies to the AGASA, HiRes, and Auger experiments; the second limit becomes relevant for the EUSO experiment. Valid when $N \gg n \gg 1$, one has:

$$P(\{m_i\}, n, N) \approx \mathcal{P} \left[\prod_{j=2} \frac{(\overline{m}_j)^{m_j}}{m_j!} e^{-\overline{m}_j r^j (j-2)!} \right], \quad (14)$$

where $r \equiv (N - m_0)/n \approx 1$, and the prefactor (nearly unity) \mathcal{P} is

$$\mathcal{P} = e^{-(n-m_1)} \left(\frac{n}{m_1} \right)^{m_1 + \frac{1}{2}}. \quad (15)$$

The non-Poisson nature of Eq. (14) is reflected in the factorials and powers of r in the exponents, and the deviation of the prefactor from unity.

In the case where $n > N \gg 1$, higher j -plets are common and the distribution of clusters can be rather broad in j . We may write \overline{m}_j in the approximate form:

$$\overline{m}_j \approx \sqrt{\frac{N^3}{2\pi en}} \left(\frac{en}{jN} \right)^{j + \frac{1}{2}}. \quad (16)$$

Extremizing this expression with respect to j , one learns that the most populated j -plet occurs near $j \sim n/N$. Combining this result with the broad distribution expected for large n/N , one expects clusters with j up to several $\times \frac{n}{N}$ to be common in the EUSO experiment.

Shown in Fig. 5 is an assessment²⁴ of the AGASA-plets, five doublets plus a triplet, obtained using formula (14). Two features of the figure are noteworthy. The first is the rather extreme sensitivity of the statistical significance to the angular binning size. AGASA claims a 2.5° resolution, which puts the significance of their clusters at 10^{-3} . If the resolution were 3° (2.0°), the significance would be a factor of six weaker (fifteen stronger). The second feature is the factor of a few error made when Poisson statistics are blindly applied.

The explicit dependence of random clustering probabilities on angular bin-size presented here may prove quite useful in the future. If clustered events originated from a common source and traveled without bending, then the experimental angular resolution is the optimal bin-size. On the other hand, if clustering results from

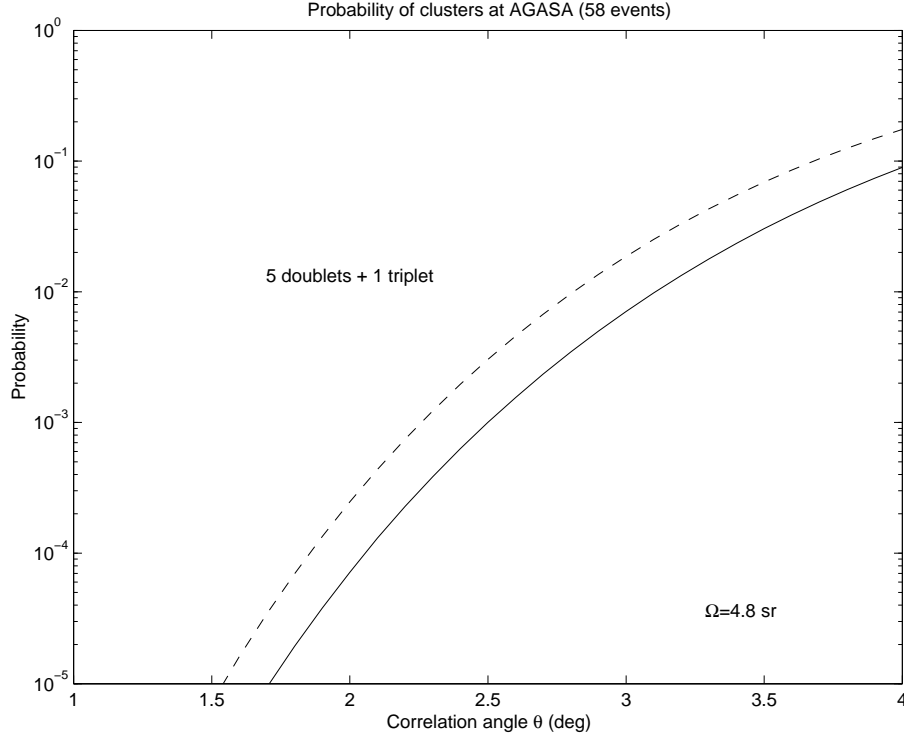


Figure 5. Exact (solid) and Poissonian (dashed) inclusive probabilities (from ref. 24) for five doublets and one triplet in the 58-event AGASA sample.

magnetic focusing, then the angular size of magnetic caustics may be the relevant bin-size. If clustering results from density fluctuations in the Galactic halo, then the angular size of these fluctuations may be the optimal bin-size. Since photons are not bent by magnetic fields whereas protons are bent, the optimal bin-size for photon-initiated events is likely smaller than that for proton-initiated events. The analytic formulas are easily applied to any chosen angular bin-size.

6 Z-bursts

A rather conservative and economical solution proposed to solve the super-GZK mysteries is the Z-burst mechanism. Here, EECR neutrinos scattering resonantly on the cosmic neutrino background (CNB) predicted by Standard Cosmology, to produce Z-bosons.²⁵ These Z-bosons in turn decay to produce a highly boosted “Z-burst”, containing on average twenty photons and two nucleons above E_{GZK} (see Fig. 6). The photons and nucleons from Z-bursts produced within 50 to 100 Mpc of earth can reach earth with enough energy to initiate the air-showers observed at $\sim 10^{20}$ eV. The energy of the neutrino annihilating at the peak of the Z-pole is

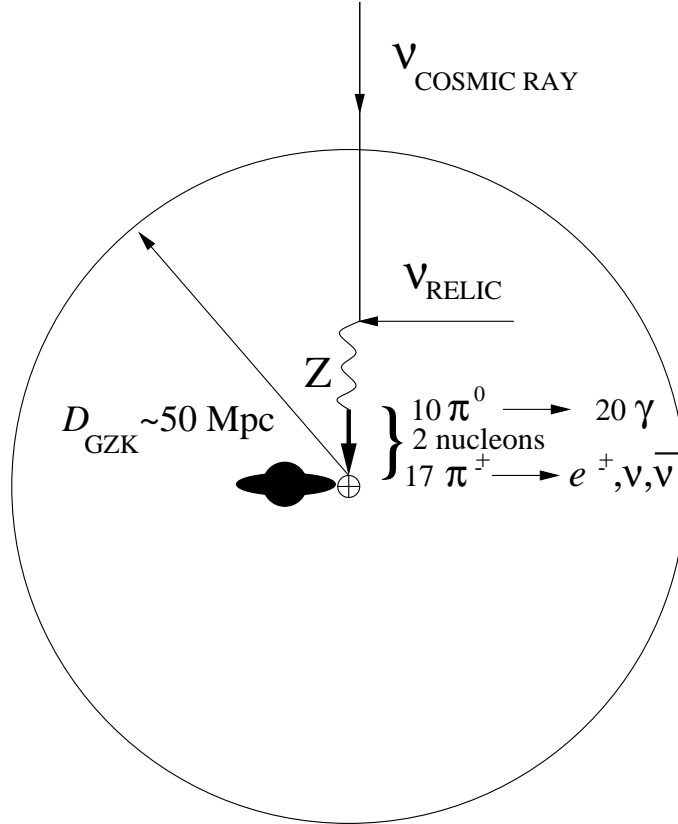


Figure 6. Schematic diagram showing the production of a Z-burst resulting from the resonant annihilation of a cosmic ray neutrino on a relic (anti)neutrino. If the Z-burst occurs within the GZK zone (~ 50 to 100 Mpc) and is directed toward the earth, then photons and nucleons with energy above the GZK cutoff may arrive at earth and initiate super-GZK air-showers

$$E_{\nu_j}^R = \frac{M_Z^2}{2m_j} = 4 (eV/m_j) \text{ ZeV}. \quad (17)$$

The resonant-energy width is narrow, reflecting the narrow width of the Z-boson: at FWHM $\Delta E_R/E_R \sim \Gamma_Z/M_Z = 3\%$. The mean energies of the ~ 2 baryons and ~ 20 photons produced in the Z decay are easily estimated, when the Z-burst energy is averaged over the mean multiplicity of 30 secondaries in Z-decay. The photon energy is reduced by an additional factor of 2 to account for their origin in two-body π^0 decay.

In the simplest approximation, the spectrum of arriving nucleons is

$$\frac{dN}{dE} \sim \frac{1}{D^2} \times \frac{dN}{dD} \times \frac{dD}{dE} \propto E^{-1} \quad (18)$$

from sources uniformly distributed out to

$$D_{\text{GZK}} \sim \lambda \frac{\ln\left(\frac{N E_{\text{GZK}}}{E^R}\right)}{\ln(1-f)}, \quad (19)$$

with a pileup at E_{GZK} resulting from all primaries originating beyond this distance. The E^{-1} spectrum extends from E_{GZK} out to the maximum nucleon energy $\sim E^R/30 \sim 10^{21}(\frac{0.1\text{eV}}{m_\nu})$ eV. More realistic simulations including energy-loss processes, cosmic expansion, and boosted Z-boson fragmentation functions give a softer spectrum, but a characteristic feature of the Z-burst mechanism remains that the super-GZK spectrum is considerably harder than the sub-GZK spectrum having power law index -2.7.

The necessary conditions for the viability of this model are then, a neutrino mass scale of the order 0.1 to 1 eV, and a sufficient flux of neutrinos at $\gtrsim 10^{21}$ eV.²⁵ The second condition seems challenging, while the first is quite natural in view of the recent neutrino oscillation data. Fits to atmospheric neutrino data yield $m_\nu \geq \sqrt{\delta m_{\text{atm}}^2} \sim 0.05$ eV. A recent estimate²⁶ of the total neutrino mass in the Universe, based on the distribution of large-scale structures, is $\sum_j m_j \sim 2$ eV. Most recently, the WMAP collaboration ambitiously combined their new CMB data with matter-distribution spectra to deduce²⁷ $\sum_j m_j \lesssim 0.71$ eV. However, omission of the suspect Lyman-alpha data from the analysis returns one to $\sum_j m_j \lesssim 1$ eV, with dependence on priors²⁸. And so it appears that the neutrino mass is squeezed to lie within just the 0.1 to 1.0 eV range most beneficial to the Z-burst model!²⁹

What is not known is whether Nature has provided the large neutrino flux at energy E^R to allow an appreciable event rate in future EECR detectors. It is conceivable, although unlikely, that the flux is so large that present EECR events are initiated by Z-bursts. A recent analysis³⁰ of this possibility gave a best fit with $m_\nu = 0.26_{-0.14}^{+0.20}$ eV, nicely consistent with the WMAP bound. Another analysis³¹ fits the EECR spectrum down to the ankle with Z-burst generated events and a neutrino mass of $\sqrt{\delta m_{\text{atm}}^2} \sim 0.07$ eV, again in accord with the WMAP bound. The flux requirements for the Z-burst mechanism can be ameliorated if there is an overdensity of relic neutrinos, as would happen if (i) there was a significant chemical potential, or (ii) neutrinos were massive enough to cluster in “local” structures such as the Galactic SuperCluster. Large chemical potentials have been ruled out recently³², and this exclusion is confirmed by the WMAP data. Local clustering has been studied,³³ with the conclusion being that a significant overdensity on the SuperCluster scale requires a neutrino mass in excess of 0.3 eV. Such a mass is marginally allowed by the new WMAP limit.

The large neutrino flux required at E^R to explain the AGASA super-GZK event rate with the Z-burst mechanism has engendered much debate. While the direct neutrino flux limits do not preclude such a large flux,¹⁷ limits on the associated diffuse gamma-ray flux disfavor most source mechanisms. A wide range of possible sources have been critically reviewed recently.^{34,35} Even the so-called hidden sources (which emit only neutrinos) seem problematical.³⁶ On the other hand, new possibilities have emerged for production of neutrino fluxes. Wake-fields in plasmas³⁷ may accelerate particles to energies of 10^{23} eV, and a special class of

blazars may beam neutrinos at us.³⁸ “Mirror matter” topological defects may decay to mirror neutrinos which then may oscillate into active neutrinos^{35,39}. Recombination of the strong magnetic fields surrounding black holes offers another acceleration mechanism that is still in the infancy of its exploration.⁴⁰

7 Summary and Acknowledgments

The next ten years will exploit neutrino eyes to see the extreme Universe. Theory and experiment are rapidly converging to usher in the neutrino window to astronomy, and the astronomy window into neutrino physics. Fruitful discoveries, probably beyond anything anticipated today, await us.

I acknowledge my collaborators for the joint work I have presented here. They are J. Beacom, N. Bell, G. Bhattacharyya, H. Goldberg, D. Hooper, A. Kusenko, H. Päs, S. Pakvasa, and L. Song. This work is supported by the U.S. Department of Energy grant no. DE-FG05-85ER40226, and by the Kavli ITP visitor program.

References

1. R. Protheroe, ArXiv:astro-ph/9809144 (1998).
2. R. Engel, D. Seckel, T. Stanev, Phys. Rev. D **64** (2001) 093010.
3. M. Nagano and A. A. Watson, Rev. Mod. Phys. **72** (2000) 689.
4. D. De Marco, P. Blasi, and A. Olinto, ArXiv: astro-ph/0301497.
5. Webpages for EUSO are available at <http://www.euso-mission.org> and <http://aquila.lbl.gov/EUSO/>
6. C. Barbot and M. Drees, Phys. Lett. B **533** (2002) 107; C. Barbot, M. Drees, F. Halzen, and D. Hooper, Phys. Lett. B **555** (2003) 22 [ArXiv:hep-ph/0207133 (2002)].
7. T. W. Kephart and T. J. Weiler, Astropart. Phys. **4** (1996) 1271 [ArXiv:astro-ph/9505134]; S. Wick, T. Kephart, T. Weiler, and P. Biermann, Astropart. Phys. **18** (2003) 663 [ArXiv:astro-ph/0001233].
8. T. Abu-Zayyad et al. (HiRes Collaboration), ArXiv:astro-ph/0208301.
9. G. Hou and M. Huang, ArXiv:astro-ph/0204145.
10. J. Beacom, N. Bell, D. Hooper, S. Pakvasa, and T. J. Weiler, ArXiv:hep-ph/0211305, to appear in Phys. Rev. Lett.; some earlier papers on cosmic tests of neutrino decay are S. Pakvasa, Lett. Nuovo Cim. **31**, 497 (1981); Y. Farzan and A. Y. Smirnov, Phys. Rev. D **65**, 113001 (2002); T. J. Weiler, W. A. Simmons, S. Pakvasa and J. G. Learned, arXiv:hep-ph/9411432; P. Keranen, J. Maalampi and J. T. Peltoniemi, Phys. Lett. B **461**, 230 (1999).
11. J. F. Beacom and N. F. Bell, Phys. Rev. D **65**, 113009 (2002).
12. A. Kusenko and T. J. Weiler, Phys. Rev. Lett. **88** (2002) 161101.
13. J. Feng, P. Fisher, F. Wilczek, and T. Yu, Phys. Rev. Lett. **88** (2002) 161102.
14. G. Burdman, G., F. Halzen, and R. Ghandi, Phys. Lett. B **417** (1998) 107.
15. Z. Fodor, S. D. Katz, A. Ringwald, and H. Tu, ArXiv: hep-ph/0303080.
16. A. Olinto, C. Tyler, and G. Sigl, Phys. Rev. D **63** (2001) 055001.
17. L. Anchordoqui, J. Feng, H. Goldberg, and A. Shapere, ArXiv:hep-ph/0207139., to appear in Phys. Rev. D.

18. H. Goldberg and T. J. Weiler, Phys. Rev. D59 (1999) 113005.
19. H. Goldberg, L. G. Song, and T. J. Weiler, in preparation.
20. M. Takeda et al. (AGASA Collaboration), Proc. ICRC 2001, Hamburg, Germany, updates Y. Uchihori et al., Astropart. Phys. 13 (2000) 151.
21. P. Tinyakov and I. Tkachev, Astrophys. J. 577 (2002) L93 [ArXiv:astro-ph/0204360]; *ibid.*, JETP Lett. 74 (2001) 445.
22. H. Goldberg and T. J. Weiler, Phys. Rev. D64 (2001) 056008.
23. W. Burgett and M. O'Malley, ArXiv:hgep-ph/0301001, to appear in Phys. Rev. D.
24. L. Anchordoqui et al., Mod. Phys. Lett. 16, 2033 (2001) [arXiv:astro-ph/0106501].
25. T.J. Weiler, Phys. Rev. Lett. 49, 234 (1982); *ibid.*, Astrophys. J. 285, 495 (1984); *ibid.*, Astropart. Phys. 11, 303 (1999); E. Roulet, Phys. Rev. D47 (1993) 5247; Y. Yoshida, H. Dai, C. Jui, and P. Sommers, Astrophys. J. 479 (1997) 547; D. Fargion, B. Mele and A. Salis, Astrophys. J. 517, 725 (1999).
26. O. Elgaroy et al., 2dFGRS team, arXiv:astro-ph/0204152 and Phys. Rev. Lett. 89 (2002), to appear.
27. D. Spergel et al., ArXiv:astro-ph/0302209.
28. S. Hannestad, ArXiv:astro-ph/0303076; O. Elgaroy and O. Lahav, ArXiv:astro-ph/0303089.
29. G. Bhattacharyya, H. Päs, L. Song, and T. J. Weiler, ArXiv:hep-ph/0302191, to appear in Phys. Lett. B.
30. Z. Fodor, S. Katz, and A. Ringwald, JHEP 0206 (2002) 046; *ibid.*, Phys. Rev. Lett. 88 (2002) 171101.
31. G. Gelmini and G. Varieschi, ArXiv:hep-ph/0201273.
32. A. D. Dolgov et al., Nucl. Phys. B632 (2002) 363; K. Abazajian, J. Beacom, and N. Bell, Phys. Rev. D66 (2002) 013008.
33. C.-P. Ma and Singh, Phys. rev. D67 (2003) 023506 [ArXiv:astro-ph/0208419].
34. F. Halzen and D. Hooper, Rept. Prog. Phys. **65**, 1025 (2002); J. G. Learned and K. Mannheim, Ann. Rev. Nucl. Part. Sci. **50**, 679 (2000). O. Kalashev, V. Kuzmin, D. Semikoz, and G. Sigl, Phys. Rev. D66 (2002) 063004 [ArXiv:hep-ph/0205050].
35. V. Berezhinsky, ArXiv:hep-ph/0303091.
36. D. Gorbunov, P. Tinyakov, and S. Troitsky, Astropart. Phys. 18 (2003) 463 [ArXiv:astro-ph/0206385].
37. P. Chen, T. Tajima, and Y. Takahashi, Phys. Rev. Lett. 89 (2002) 161101.
38. A. Neronov and V. Semikoz, Phys. Rev. D66 (2002) 123003 [ArXiv:hep-ph/0208248].
39. V. Berezhinsky and A. Vilenkin, Phys. Rev. D62, 083512 (2000).
40. P. Kronberg, Q. Dufton, H. Li, and S. Colgate, ArXiv:astro-ph/0106281, to appear in Astrophys. J.